A&A, 703, A204 (2025)
https://doi.org/10.1051/0004-6361/202556562

Astronomy & Astrophysics

Lithium evolution in the Galactic thin disc from main-sequence and early red-giant-branch stars

C. T. Nguyen[1,2,⋆], G. Cescutti[1,2], F. Matteucci[1,2,3], F. Rizzuti[4,2,5], A. Mucciarelli[6,7], D. Romano[6], L. Magrini[8], A. J. Korn[9], A. Bressan[10], and L. Girardi[11]

[1] University of Trieste, Piazzale Europa, 1, Trieste, Italy
[2] INAF Osservatorio Astronomico di Trieste, Via Giambattista Tiepolo, 11, Trieste, Italy
[3] Institute for Fundamental Physics of the Universe, via Beirut, 2, 34151 Trieste, Italy
[4] Heidelberger Institut für Theoretische Studien, Schloss-Wolfsbrunnenweg 35, 69118 Heidelberg, Germany
[5] INFN, Sezione di Trieste, via Valerio 2, 34134 Trieste, Italy
[6] INAF, Osservatorio di Astrofisica e Scienza dello Spazio, Via Gobetti 93/3, 40129 Bologna, Italy
[7] Dipartimento di Fisica e Astronomia, Università degli Studi di Bologna, Via Gobetti 93/2, 40129 Bologna, Italy
[8] INAF, Osservatorio Astrofisico di Arcetri, Largo E. Fermi 5, 50125 Firenze, Italy
[9] Division of Astronomy and Space Physics, Department of Physics and Astronomy, Uppsala University, Box 516, 75120 Uppsala, Sweden
[10] SISSA, Via Bonomea 265, 34136 Trieste, Italy
[11] INAF – Osservatorio Astronomico di Padova, Vicolo dell'Osservatorio 5, Padova, Italy

Received 23 July 2025 / Accepted 25 September 2025

ABSTRACT

The role of novae as producers of galactic lithium-7 (Li) has been suggested since the 1970s, and it has been reconsidered recently with the detection of beryllium-7 in their outbursts. At the same time, stellar models are moving forward to help us understand the discrepancy between the primordial Li abundance predicted by the standard Big Bang nucleosynthesis theory and the measured value of old dwarf stars. For this work, we followed the evolution of Li in the Galactic thin disc starting from a primordial value of A(Li)= 2.69 dex and applying Li depletion corrections of the stellar model with overshoot to our chemical evolution models. We used the upper envelope of the observational data to constrain the models. In addition to the dwarf main-sequence (MS) stars, our analysis included, for the first time, the early red-giant-branch (RGB) stars. In addition to the renowned Spite plateau of the MS stars at low metallicities, we also confirm the existence of a second A(Li) plateau of the early RGB stars, which can be explained by our model with the corrections from stellar models. Our best-fit model was obtained with an effective averaged Li yield $^{Li}Y_{\rm Nova} = 2.34 \times 10^{-5}\,{\rm M}_{\odot}$ during the whole lifetime of a nova. This reinforces the possibility that novae are the main galactic Li source, together with the stellar models' ability to resolve the 'cosmological Li problem' in this context.

Key words. nuclear reactions, nucleosynthesis, abundances – stars: abundances – novae, cataclysmic variables – Galaxy: abundances – Galaxy: evolution

1. Introduction

Tracing galactic lithium-7 (Li) provides abundant information on the evolution of the Milky Way (for example, Matteucci et al. 1995; Travaglio et al. 2001; Prantzos 2012, and references therein). Most of the models included novae as the primary Li factory (D'Antona & Matteucci 1991; Romano et al. 1999), but for a long time there was no observational evidence supporting Li production in nova outbursts.

Since the discovery of Tajitsu et al. (2015), where Be was detected in the classical Nova Delphini 2013, classical nova explosions were confirmed to be the main source of the galactic Li production among other possible sources such as red-giant or asymptotic-giant-branch (AGB) stars. Briefly after that, Izzo et al. (2015) reported the detection of the Li I line at $\lambda = 6708$ Å in the spectra of Nova Centauri 2013 (V1369Cen). This was further supported by the detection of the isotope Be in many other novae (Molaro et al. 2016; Tajitsu et al. 2016; Izzo et al. 2018; Molaro et al. 2020b; Arai et al. 2021; Molaro et al. 2022, 2023). Currently, a possible detection of a 478 keV emission line emitted in the Be decay into Li has been reported by Izzo et al. (2025) for V1369Cen. This is due to the short lifetime of Be (~53 days) and its decay into Li. The amount of ejected Li per nova event, $\approx 1\text{–}10 \times 10^{-9}\,{\rm M}_{\odot}$, was determined in these cases. This strongly indicates that the main source of Li production in the Milky Way is from nova systems.

Over the last decade, observational surveys have provided a huge amount of data on Li abundances, from Galactic discs to the bulge, from star clusters to halo field stars, from the main sequence (MS) to the advanced red-giant and asymptotic-giant-branch evolutions. For example, the Gaia-ESO survey (Fu et al. 2018; Randich et al. 2020; Magrini et al. 2021; Romano et al. 2021), the Galactic Archaeology with HERMES survey (GALAH, De Silva et al. 2015; Wang et al. 2024), the Large Sky Area Multi-Object Fiber Spectroscopic Telescope survey (LAMOST, Gao et al. 2019; Ding et al. 2024), and the upcoming 4MOST MIlky way Disc And BuLgE High-Resolution survey (4MIDABLE-HR, Bensby et al. 2019). These surveys are a great source of observational data for chemical evolution models to study precisely the properties of galactic Li evolution.

⋆ Corresponding author: chi.nguyen@inaf.it

In particular, various models have recently claimed the importance of novae for the enrichment of Li in the solar neighbourhood, for example Cescutti & Molaro (2019), Romano et al. (2021), Gao et al. (2024), and Borisov et al. (2024). These works agree that novae are the main source of the galactic Li production. However, the precise amount of Li yield per nova event differs between the different works. In particular, Cescutti & Molaro (2019) claimed an amount of 1.8×10^{-9} $M_\odot$ to be the best constrained value (assuming that about 10^4 explosion events occur during the whole lifetime of a nova), while Borisov et al. (2024) claimed a value about three times higher, 5×10^{-9} $M_\odot$, with their one-zone model (assuming an average mass of the ejecta of 5×10^{-5} $M_\odot$ in a nova lifetime). Furthermore, the dependence of the nova Li yield on other physical parameters such as metallicity, ejecta mass, and delay time gives rise to the complexity of nova treatment in galactic chemical evolution models (see Kemp et al. 2022, 2024, and references therein for more details).

On the other hand, observations of metal-poor dwarf MS stars ([Fe/H] ≤ -1) indicate an A(Li) plateau commonly known as the Spite plateau (A(Li) $\approx$ 2.2 dex; Spite & Spite 1982a,b; Bonifacio 2002; Charbonnel & Primas 2005; Korn et al. 2007). This measured value is approximately three times smaller than the predicted primordial value obtained from Big Bang nucleosynthesis studies (A(Li) $\approx$ 2.7 dex; Coc et al. 2014; Cyburt et al. 2016; Singh et al. 2019; Iliadis & Coc 2020; Pitrou et al. 2021; Singh et al. 2024) assuming the cosmological parameters determined by Planck (Planck Collaboration XVI 2014). The origin of this discrepancy is still debated, and is usually known as the 'cosmological Li problem'. For example, Eggenberger et al. (2012), Fu et al. (2015), and Nguyen et al. (2025a) proposed different mechanisms involving Li depletion during the PMS evolution, while Richard et al. (2005) moderated atomic diffusion with turbulent mixing during the MS. Recently, Nguyen et al. (2025a) presented a grid of stellar models in which the envelope overshoot efficiency parameter was modified during the PMS evolution of the stars to better understand this issue. Their models were calibrated with the well-studied globular cluster NGC 6397. Taking advantage of the provided stellar grid, we explored the amount of stellar Li depletion relative to the primordial value (A(Li) = 2.69 dex), and coupled it with the predictions of our chemical evolution code. For the purpose of this work, we adopted the simplified treatment of nova Li yield from Cescutti & Molaro (2019) and introduced a correction term accounting for stellar Li depletion due to the evolution of stars.

Moreover, Mucciarelli et al. (2022) recently discovered a thin plateau among the metal-poor red-giant-branch (RGB) stars. Their sample contains 58 early RGB stars with metallicity ranges $-7 \leq$ [Fe/H] ≤ -1.3, and high-resolution spectra were used for the derivation of A(Li). The authors discovered a plateau for these early RGB metal-poor stars, with mean value A(Li) = 1.09 ± 0.08 dex, that exhibits a trend similar to that of MS stars (or the so-called Spite plateau; Spite & Spite 1982a,b). Hence, for this work we also studied the behaviour of A(Li) at this early RGB evolution to investigate this discovered plateau and the role of nova production in Li enrichment at this evolutionary stage. For this purpose, we selected two subsamples of dwarf MS and early RGB stars from the recent catalogues of GALAH DR4 (Wang et al. 2024) and Gaia-ESO (Magrini et al. 2021; Romano et al. 2021), complemented with the sample of F- and G-type dwarf MS stars from Bensby & Lind (2018).

The paper is organised in six sections. In Sect. 2 we describe the methodology used to select our data samples from the big surveys GALAH and Gaia-ESO. Section 3 shows the predictions from the stellar models regarding the depletion of A(Li) relative to the primordial value. In Sect. 4, we describe the chemical evolution model that is used for this work. We present the obtained results in Sect. 5, and draw our conclusions in Sect. 6.

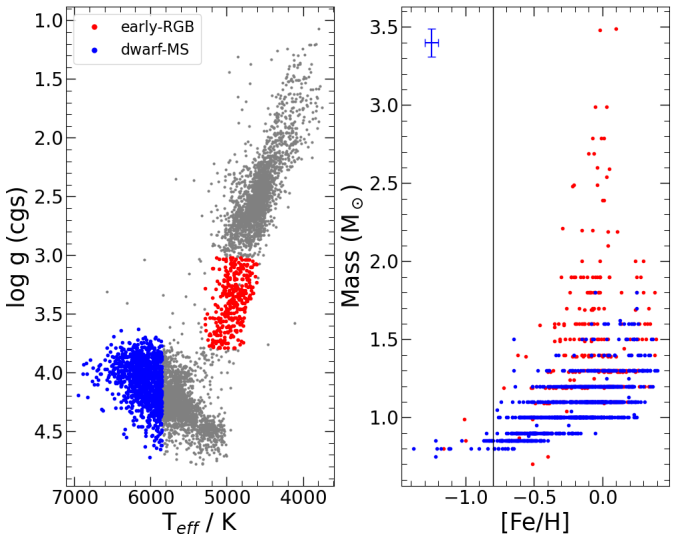

Fig. 1. Left panel: sample of 7347 field stars from Magrini et al. (2021), with our selected subsamples highlighted in red and blue. Right panel: mass distribution with metallicity ([Fe/H]) of stars in our selected samples. The blue error bar indicates the mean uncertainty value of our selected dwarf MS sample. The black vertical line marks [Fe/H] = −0.8 dex.

2. Sample selection

The catalogue of Magrini et al. (2021) presents high-quality data from the Gaia-ESO iDR6 survey. It contains 7347 field stars with metallicity in the range $-1 \leq$ [Fe/H] ≤ 0.5 dex. The Li abundances are derived with the one-dimensional (1D) local thermodynamic equilibrium (LTE) assumption (Franciosini et al. 2022). We selected two subsamples of dwarf MS stars ($\log g > 3.6$ and $T_{\rm eff} \geq 5850$ K) and early RGB stars ($3.1 \leq \log g \leq 3.8$ and $4600 \leq T_{\rm eff}/{\rm K} \leq 5300$) for our analysis in this work. The choice of $\log g$ and $T_{\rm eff}$ was made to avoid the stars that are going through Li depletion due to convective-driven and thermohaline mixing. The selected samples are shown in the left panel of Fig. 1. We note that we already excluded Li-rich stars from our samples in Fig. 1, based on the definition found in Magrini et al. (2021), namely A(Li) $\geq$ 2.0 dex, $3800 \leq T_{\rm eff}/{\rm K} \leq 5000$, $\log g \leq 3.5$, and the gravity index $\gamma \geq 0.98$. Furthermore, the mass of each star is reported in the Gaia-ESO catalogue (see Magrini et al. 2021). We show in the right panel of Fig. 1 the mass distribution of stars in the two subsamples. In particular, the metal-poor stars ([Fe/H] ≤ -0.8) are in fact low-mass stars with masses of approximately 0.8 $M_\odot$. Within the uncertainty, they appear to be consistently below 1 $M_\odot$. This motivated us to explore the correction from available stellar models on the variation of Li abundances, which is described in the next section. We also adopted the catalogue from Romano et al. (2021) that includes 26 carefully selected open clusters, and 3 210 field stars from the Gaia-ESO iDR6 survey. This sample also contains important information, such as the stellar ages and galactocentric distances. We applied the same selection method as for the previous sample, meaning $\log g > 3.6$ and $T_{\rm eff}/K \geq 5850$.

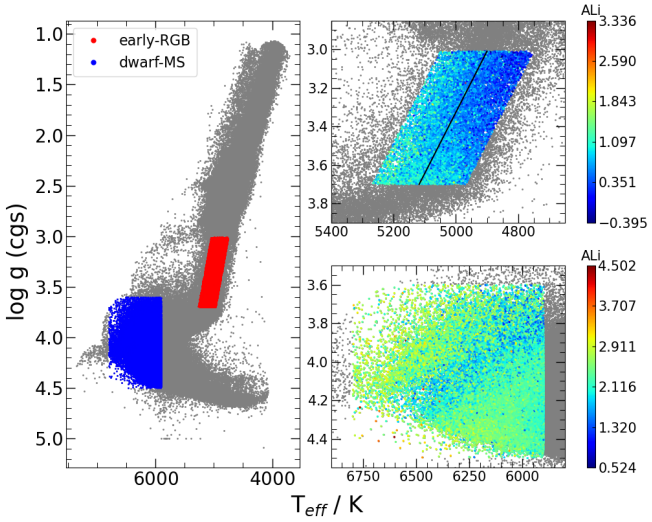

Fig. 2. Left panel: complete sample of Li detection adopted from the GALAH DR4 catalogue (grey dots). Our two selected samples are highlighted in blue and red. Top right panel: zoomed-in region of our selected early RGB stars sample, with the colour bar indicating A(Li). Bottom right panel: our sample of selected dwarf MS stars (see text for details of the selections).

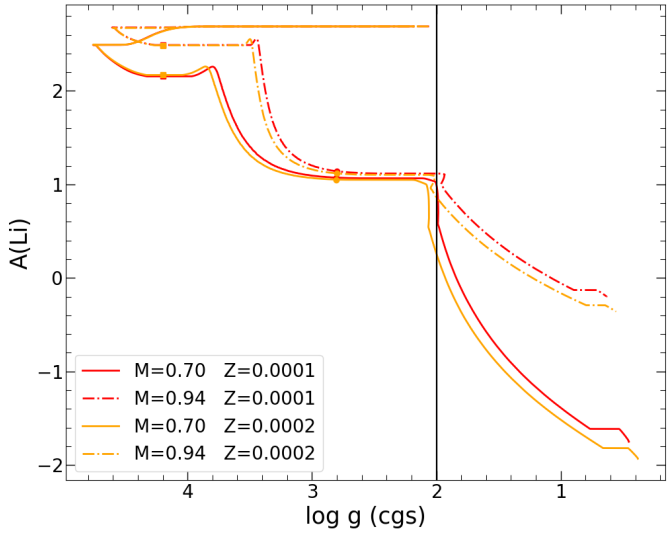

Fig. 3. Variation in surface Li abundance with $\log g$ of four selected stellar models. The square marks the location where $\log g \sim 4.1$ on the MS, while the circle indicates $\log g \sim 2.8$ on the early RGB. The black line indicates $\log g \sim 2$ around the RGB bump.

The GALAH survey also provides us with another opportunity to study the chemical history of the Milky Way using high-resolution spectroscopy. Lithium is one of the main focuses of the survey; Wang et al. (2024) provided 3D non-LTE (3D-NLTE) Li abundances for 581 149 field stars released in GALAH DR3 (Buder et al. 2021). For this work we adopted the catalogue with three additional conditions for our selected samples. They are with flags: (i) `flag_ALi` = 0, which means only 228 613 field stars with actual Li detection are used; (ii) `flag_fe_h` = 0 and (iii) `flag_sp` = 0, which mean no problems noted from the observational analysis. The full sample is presented in the left panel of Fig. 2. Our subsamples for the dwarf MS and the early RGB stars are highlighted in blue and red, respectively. First, for the dwarf MS sample, we selected stars with $3.6 < \log g < 4.5$ and $5850 \leq T_{\rm eff}/{\rm K} \leq 6800$. The choices of $\log g$ and $T_{\rm eff}$ were made to avoid the contamination from stars that are undergoing the convection-driven Li depletion. We obtained about 97 193 stars for this subsample, which are shown in the bottom right panel of Fig. 2. Then, for our early RGB stars, to avoid distraction from the red clump stars, we selected stars with $3.0 < \log g < 3.7$. After that, within the narrow region $4500 < T_{\rm eff} < 5500$ K, we searched for the synthetic line that mimics the RGB evolution in this region by using the simple `polyfit` Python function, shown as the black line in the top right panel of Fig. 2. We then selected the stars within the range of $T_{\rm eff}^{synthetic} \pm 150$ K for our early RGB sample. As a result, we obtained about 15 316 RGB stars for the sample.

Furthermore, we adopted the catalogue from Bensby & Lind (2018), which contains in total 714 F- and G-dwarf, turn-off, and subgiant stars. Their Li abundances were derived with 1D-LTE analysis of high-resolution spectra. For our sample, we selected only 275 stars with the actual detected Li abundances and $T_{\rm eff} \geq 5850$ K.

3. Predictions from stellar models

Nguyen et al. (2025a) introduced stellar models with different values of the envelope overshoot efficiency parameter between the pre-main-sequence and post-main-sequence evolutions to reproduce the Li plateau on the MS and the RGB bump location of the GC NGC 6397, using the PARSEC code (see also Bressan et al. 2012; Nguyen et al. 2022, 2025b, for more information). In particular, a value of $\Lambda_{\rm e} = 0.6 H_p$ is applied to the post-MS evolution to calibrate the RGB bump, and a smaller value, $\Lambda_{\rm e}^{\rm p} = 0.05$–$0.6 H_p$ (dependent on the initial masses) is applied to the early PMS evolution, where H_p is the pressure scale height. As a result, a depletion from the primordial value (A(Li) = 2.69 dex; Coc et al. (2014), adopted as the initial value applied to the stellar models) to the measured value in dwarf, turn off, and subgiant stars of NGC 6397 (A(Li) $\approx$ 2.22 dex; Lind et al. 2009) is obtained.

As mentioned above, the observed metal-poor stars ([Fe/H] ≤ -0.8) show a mass range of approximately 0.8–1.0 $M_\odot$. Meanwhile, Nguyen et al. (2025a) provides models with $M \sim 0.7$–$0.94\,M_\odot$ for two metallicity sets $Z = 0.0001, 0.0002$ ([Fe/H] $\approx -2.4, -2.1$). We show the variation of A(Li) with $\log g$ for four selected models at the limit of the sets in Fig. 3. All models evolve from the PMS (starting at $\log g \sim 2.2$, A(Li) = 2.69) towards higher $\log g$ and make the turning point at the zero-age MS (ZAMS). The variation in A(Li) during this phase shows a clear depletion due to the efficiency of the envelope overshoot, which mainly depends on mass. Subsequently, atomic diffusion causes further depletion of A(Li) from the ZAMS until the end of the MS, where mixing partially restores it. The square symbol marks the location where diffusion shows its maximum efficiency. Subsequently, the convective envelope penetrates towards the inner layers, which leads to the dilution of Li in the envelope. This dilution process leads to a significant depletion during this evolutionary phase until it reaches a constant value when the first dredge-up (1DU) is completed in the RGB phase (dotted symbols). Thermohaline mixing becomes active and depletes even more A(Li) in the more advanced evolution above the RGB bump (see also Charbonnel & Zahn 2007, and references therein).

In Fig. 4, we show the depletion of Li abundance from the initial value (A(Li) = 2.69 dex) at the MS ($\log g \sim 4.1$) and at the RGB (before the RGB bump) when the 1DU is already completed ($\log g \sim 2.8$). The theoretical prediction indicates an

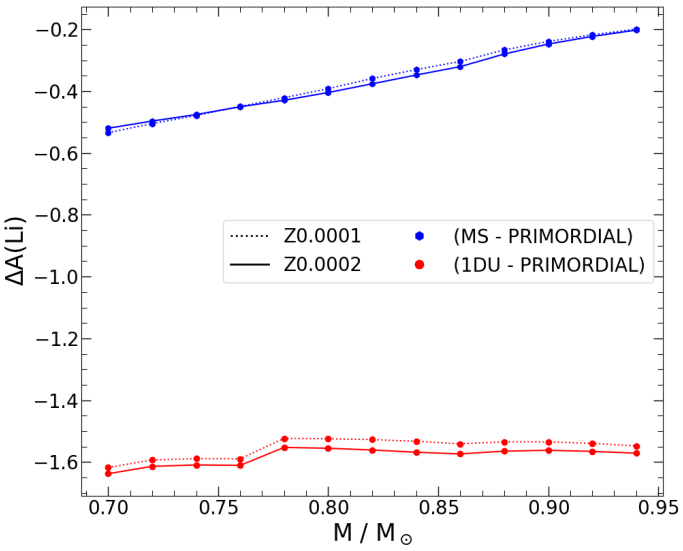

Fig. 4. Depletion of Li abundance up to the MS (blue) and after the 1DU at the early RGB phase (red). The models are from Nguyen et al. (2025a), including the depletion during the PMS phase due to the envelope overshoot.

overall depletion from the initial value throughout the entire evolution of the stars. Firstly, within the presented mass and metallicity ranges, a depletion of ∼0.2–0.5 dex is seen at the MS phase, starting from the primordial value. Especially in the mass range $\leq 0.8\,M_\odot$, the model prediction shows a depletion of ∼0.4–0.5 dex, which is the typical value that is needed to reproduce the Spite plateau (A(Li) ≈ 2.2 dex; Spite & Spite 1982a,b) from the cosmologically determined value.

Secondly, within the typical uncertainty (≈0.1 dex), the depletion after the 1DU from the initial value shows an approximately constant value, i.e. ΔA(Li) ≈ 1.6 dex for all the shown models. This prediction might indicate the existence of a second plateau that is located at the early RGB evolution, where the stars have not yet been affected by thermohaline mixing, which confirms the observational results obtained by Mucciarelli et al. (2022). This aspect will be discussed in the results section below.

4. Chemical evolution model

4.1. Model for thin disc

In order to study the Li evolution of the thin disc of the Milky Way, we adopted the model introduced by Cescutti & Molaro (2019). We refer to Cescutti & Molaro (2019) for more details about the model, while we here only summarise the main ingredients for our work. In particular, the initial mass function (IMF) is adopted from Kroupa (2001), and the stellar lifetime follows Meynet & Maeder (2002). The single degenerate scheme for the progenitors of SNe Ia is adopted from Matteucci & Greggio (1986). We assume the thin disc to be formed by slow gas infall (for details see Cescutti & Molaro 2019).

The key ingredient of this model for Li is the assumption that nova systems are the principal producers of Li, although we also consider a small contribution from cosmic rays (see Prantzos 2012). The nova rate is computed by assuming the same delay time distribution function (DTD) of the SNe Ia deriving from cataclysmic variables (single degenerate scenario) as in Matteucci & Greggio (1986), but with an additional time delay to allow for the cooling of the white dwarfs.

In Cescutti & Molaro (2019), it was assumed that only binary systems formed by stars in the mass range $M = 0.8$–$8\,M_\odot$ can develop nova systems. The probability of forming a binary system of a certain mass is weighted on the IMF. The configurations of primary and secondary stars are defined by

$$f(\mu) = 2^{1+\gamma}(1+\gamma)\mu^{\gamma}, \quad (1)$$

where $f(\mu)$ is the distribution function for the mass fraction of the secondary star; $\mu = M_2/M_B$, where M_2 is the mass of the secondary star and M_B is the mass of the binary system. The exponential coefficient $\gamma = 2$ is adopted from Greggio & Renzini (1983).

The fraction of binary systems that develop a nova thus becomes a crucial parameter in the model. This parameter is defined by $N_{\rm lithium}$. In this work we use the proposed fraction by Cescutti & Molaro (2019), i.e. $N_{\rm lithium} = 0.03$, which corresponds to a Galactic rate of nova bursts of ∼20–30 $\rm yr^{-1}$ (see Shafter 1997; Della Valle & Izzo 2020).

The time when Li production takes place is defined as the time at which the primary star evolves into a white dwarf plus a delay time, $\tau_{\rm nova}$. In particular, $\tau_{\rm nova}$ is the time needed for a white dwarf to ignite the first nova outburst, which can occur only after the cooling of the white dwarf. Cescutti & Molaro (2019) found $\tau_{\rm nova} = 1$ Gyr to be the best constrained value, and in agreement with the previous works (e.g. Romano et al. 2001; Izzo et al. 2015), thus we adopted this value for this work.

The total Li produced by a nova during its lifetime is defined as ${}^{Li}Y_{\rm Nova}$. The assumption that all novae produce the same amount of Li in all events is also adopted in this work. A value of ${}^{Li}Y_{\rm Nova} = 1.8 \times 10^{-5}\,M_\odot$, with a typical number of 10^4 outbursts events during the entire lifetime of a nova (Ford 1978), is also suggested in the model of Cescutti & Molaro (2019), where they assumed the measured Li abundance from the dwarf halo stars, A(Li) = 2.28 dex, as the initial gas composition. For many years this abundance was assumed to be the primordial value until the Wilkinson Microwave Anisotropy Probe (WMAP) and Planck satellites suggested that the primordial Li abundance is three times higher (A(Li) = 2.69 dex, e.g. Cyburt et al. 2003; Coc et al. 2004).

The predicted evolution of A(Li) with metallicity [Fe/H] is shown in Fig. 5. It is clear that since Li is mainly produced by novae on long timescales, the abundance of Li for [Fe/H] < −1 is the initial value, which could be adopted as either the primordial value or the measured Spite plateau value. On the other hand, the contribution from nova explosions is dominant in the more metal-rich region. It is worth noting that the chemical evolution model predicts the evolution of Li in the interstellar medium, and when we compare our results with the Li abundance measured in the atmospheres of stars, we assume that it has not been depleted, and therefore our aim is to reproduce the upper envelope of the data. However, if the Li has indeed been depleted, this comparison should take the depletion into account. In the figure, we show models starting from an initial Li abundance as observed in halo stars (2.28 dex) and models starting with the primordial Li suggested by Planck (2.69 dex). The comparison between models with the same ${}^{Li}Y_{\rm Nova}$ but different original A(Li) values shows a clear trend of convergence towards higher metallicity. This means that the production of novae overcomes the difference in original abundances as the galaxy evolves. However, if a model with the primordial Li as its original composition, and a depletion due to the evolution of stars is assumed (dotted line), a higher nova Li yield is required to reproduce the prediction of the model with a lower original A(Li). This was suggested in

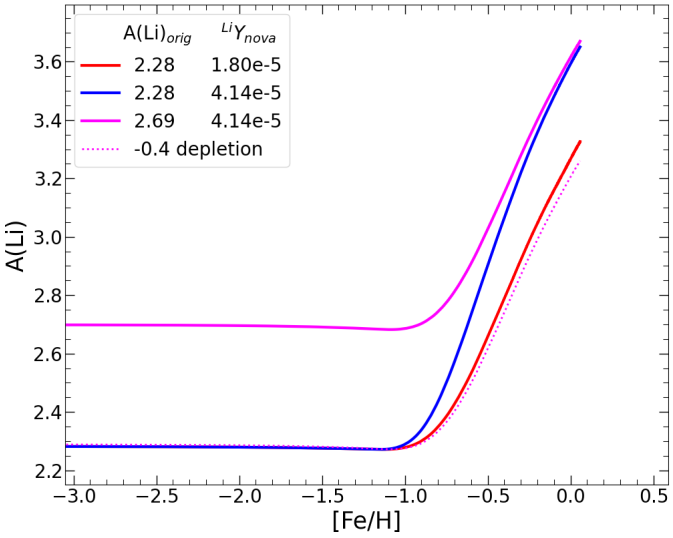

Fig. 5. Chemical evolution models of Li with different adopted values of original Li abundance and novae yields, as listed in the figure legend. An illustration model with −0.4 dex depletion from the primordial A(Li) = 2.69 model (magenta line) is plotted as the dotted line.

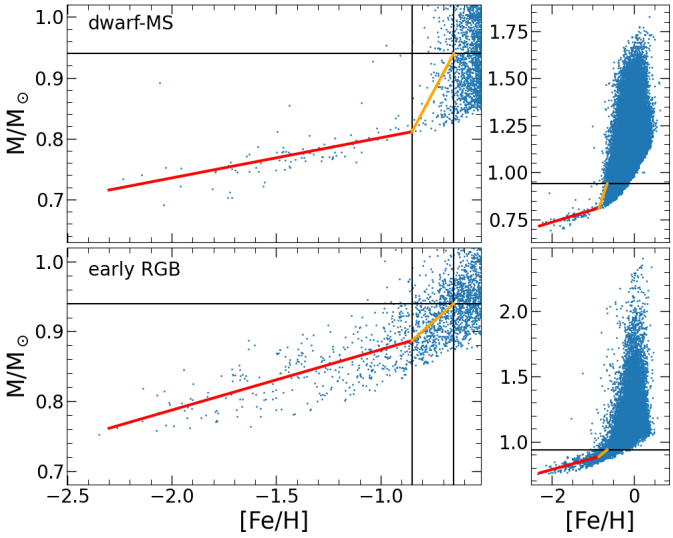

Fig. 6. Mass distribution with metallicity in two samples of dwarf MS stars (top panel) and early RGB stars (bottom panel) selected from the GALAH catalogue. The left panels zoom in on the low-mass and metal-poor area. The right panels show the whole sample. The empirical relations at two regions of [Fe/H] are shown as red and orange solid lines. The black horizontal line indicates the mass limit 0.94 $M_\odot$, while the vertical lines indicate the metallicity [Fe/H] = −0.85 and −0.65.

Cescutti & Molaro (2019), where $^{Li}Y_{\rm Nova} = 4.14 \times 10^{-5}\,M_\odot$ was obtained by using the primordial A(Li) as the original abundance and assuming a fixed amount of depletion.

For this work we explored the model computed with the primordial Li abundance, A(Li) = 2.69 dex, and applied the depletion corrections from stellar models provided in Nguyen et al. (2025a). In other words, the evolution of Li is expressed as

$$A(\mathrm{Li}) = A(\mathrm{Li})_{\rm CEM} + \Delta A(\mathrm{Li})_{\rm SM}, \quad (2)$$

where $A(\mathrm{Li})_{\rm CEM}$ is obtained from the chemical evolution model; the variables are the original Li abundance and the nova Li yield that applied to the model. $\Delta A(\mathrm{Li})_{\rm SM}$ is the predicted correction from stellar models, which depends on mass and metallicity, as we show below.

4.2. Correction from stellar models

As described in Sect. 3, the grid of stellar models covers the ranges of mass 0.70–0.94 $M_\odot$ and metallicity $-2.4 \leq$ [Fe/H] ≤ -2.1 are from Nguyen et al. (2025a). Within the models, a depletion $\Delta A(\mathrm{Li}) \approx 0.2$–$0.5$ dex from the primordial value (A(Li) = 2.69 dex) at the MS phase mainly depends on the stellar masses. On the other hand, a depletion of around 1.52–1.63 dex is predicted for stars at the early RGB phase, depending on mass and metallicity. Therefore, to determine the amount of depletion at a given point of the Li evolution (in the plane of A(Li) vs [Fe/H]), the metallicity and mass at this point are needed.

In Fig. 6, we show the mass distribution of the selected dwarf MS and early RGB stars from the GALAH catalogue (top and bottom panels, respectively). The figure indicates that the lowest mass in the samples is ∼0.7 $M_\odot$, which is covered by the stellar grid of Nguyen et al. (2025a). It also clearly indicates different trends between stars below and above [Fe/H] ∼ −0.75, especially in the case of dwarf MS stars. However, the stellar grid that is used in this work is limited to 0.94 $M_\odot$. Therefore, we adopted the depletion predicted by this 0.94 $M_\odot$ model for higher masses. We divided the samples into three regions: below [Fe/H] ≤ -0.85; between $-0.85 <$ [Fe/H] < -0.65; and above [Fe/H] ≥ -0.65. We used the `polyfit` function to obtain the empirical relation of mass and metallicity for the stars within the first two regions, which are plotted in red and orange in Fig. 6. As a result, we obtained the following relations:

$$M = 0.066[\mathrm{Fe/H}] + 0.867, \text{ for } [\mathrm{Fe/H}] \leq -0.85, \quad (3)$$

$$M = 0.643[\mathrm{Fe/H}] + 1.358, \text{ for } [\mathrm{Fe/H}] = [-0.85, -0.65]. \quad (4)$$

Similarly, we obtained the following relations for early RGB stars:

$$M = 0.086[\mathrm{Fe/H}] + 0.960, \text{ for } [\mathrm{Fe/H}] \leq -0.85, \quad (5)$$

$$M = 0.265[\mathrm{Fe/H}] + 1.112, \text{ for } [\mathrm{Fe/H}] = [-0.85, -0.65]. \quad (6)$$

The empirical relations above establish the relation between mass and metallicity. In other words, at a given metallicity [Fe/H] along the evolution of Li, we can deduce the mass and thus determine the amount of depletion that is predicted from the stellar grid. For this purpose, we applied the linear interpolation method in mass and metallicity from the stellar grid to obtain the predicted amount of depletion at a given point of the galactic A(Li) evolution. In this regard, it should be noted that for masses below 0.7 $M_\odot$ the predicted depletion of the 0.7 $M_\odot$ model is adopted. For masses above 0.94 $M_\odot$, the predicted depletion of the 0.94 $M_\odot$ model is adopted.

5. Results

As mentioned above, the models presented in this work adopt the primordial Li value, which is constrained by the number of baryons per photon from the WMAP satellite or the cosmological parameters determined by Planck (Komatsu et al. 2011; Coc et al. 2014), i.e. A(Li) = 2.69 dex. The models, with or without the Li depletion corrections predicted from stellar models (Sect. 3), are then directly compared to galactic field stars at two evolutionary phases, namely, the dwarf MS and early RGB (below the RGB bump), as selected in Sect. 2. Different models with varying values of original A(Li) and $^{Li}Y_{\rm Nova}$ are summarised in Table 1.

Table 1. Adopted parameters in each model.

Model	$A(Li)_{orig}$	$^{Li}Y_{Nova}$	Depletion
model C2.34a	2.69	2.34×10^{-5} $M_\odot$	No
model S1.80a	2.28	1.8×10^{-5} $M_\odot$	No
model C2.34b	2.69	2.34×10^{-5} $M_\odot$	Yes, MS
model C2.02b	2.69	2.02×10^{-5} $M_\odot$	Yes, MS
model C2.34c	2.69	2.34×10^{-5} $M_\odot$	Yes, RGB
model S1.80c	2.28	1.8×10^{-5} $M_\odot$	Yes, RGB
model C2.02c	2.69	2.02×10^{-5} $M_\odot$	Yes, RGB

Notes. Models are named according to their adopted parameters, following the format *XY.YYz*, where *X* represents the initial A(Li), either the cosmological (C) or Spite plateau (S) values; *Y.YY* is the $^{Li}Y_{Nova}/10^{-5}$ value; and *z* denotes the stellar Li depletion.

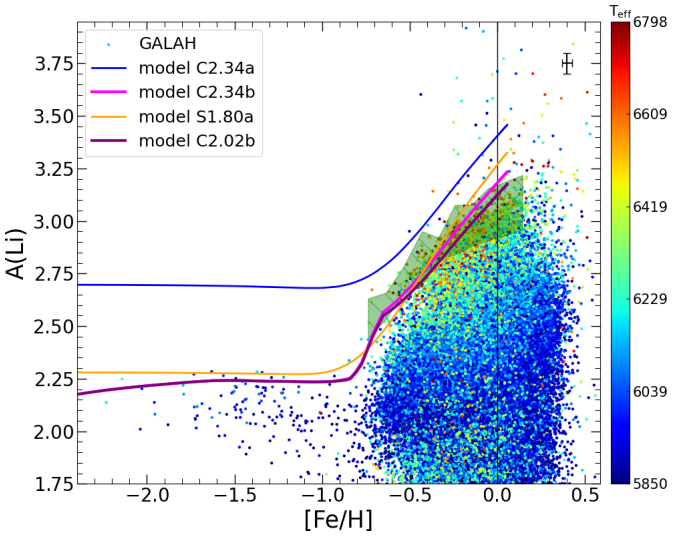

Fig. 7. Lithium abundances vs metallicity of dwarf MS stars from GALAH sample, colour-coded by their effective temperatures. Our models with and without stellar correction are shown as magenta and blue lines, respectively (see Table 1). The defined upper envelope is shown by the green shaded area. The error bars indicate the mean uncertainties of the observed data. The black vertical line marks for [Fe/H] = 0.

5.1. Dwarf main-sequence stars

First of all, we compute models with different nova Li yields, assuming the original Li abundance as A(Li) = 2.69 dex. The correction from stellar models is then added to the simulated Li abundance, following the description in Sect. 4.2.

Secondly, we define an upper envelope for the stars with [Fe/H] ≥ −0.8 dex by computing the mean value of 0.1% highest A(Li) data points in each bin over 10 bins of 0.1 dex in [Fe/H], with the minimum number of stars set to five. The envelope is then constructed by one standard deviation from the mean values of each bin, as shown in Fig. 7. Meanwhile, the large spread of A(Li) in this region might have many mechanisms at work, for instance, the stellar internal rotation and angular momentum transport processes (e.g. Eggenberger et al. 2022, and references therein), or the intrinsic properties of those stars (e.g. Dantas et al. 2025, and references therein). Additionally, there are stars with extremely high A(Li) in the region with [Fe/H] > −0.4 dex. As claimed in the literature, the origins of these stars remain unclear (see Koch et al. 2012; Gao et al. 2020). However, an investigation into these stars is beyond the scope of this paper and is worth a separate study.

As a result, Fig. 7 implies that model C2.34b, computed with the primordial value A(Li) = 2.69, $^{Li}Y_{Nova} = 2.34 \times 10^{-5}$ $M_\odot$ and taking into account the correction from stellar model, is the best-fit model. At low metallicities (−2.5 < [Fe/H] < −0.8 dex), our model reproduces very well the Spite plateau, with A(Li) = 2.15–2.25 dex. At higher metallicities, our best-fit model reproduces very well the defined upper envelope. At [Fe/H] = 0, our model shows A(Li) = 3.16 dex and a depletion of −0.22 dex predicted from stellar model, which is consistent with the measured meteoritic value, A(Li) ∼ 3.33 (Lodders et al. 2009).

The Li yield predicted by our model is in good agreement with the mean value estimated from observations of the nova beryllium-7 (Be) yield, i.e. $\sim 2.02 \times 10^{-5}$ $M_\odot$ (see Molaro et al. 2023; Izzo et al. 2025). For better comparison, we computed a model adopting this mean value, denoted as model C2.02b. As expected, the Spite plateau is unaffected by changes in the nova Li yield, while lowering the yield results in a lower Li abundance at the high-metallicity area. The discrepancy between predictions of the two models increases at higher metallicities; for example, a modest difference of ∼0.05 dex in A(Li) is seen at solar metallicity. Regardless of the modest discrepancy, both models successfully reproduce the defined upper envelope. Furthermore, the yield obtained by our best-fit model is well covered by the observed data of nova Be yields, which span from 3.4×10^{-6} to 9.7×10^{-5} $M_\odot$ (see also Molaro et al. 2016; Arai et al. 2021). This result, obtained with our model, reinforces the role of novae production in the enrichment of galactic Li. Nonetheless, we also note that our chemical evolution model employs a simple scheme to take into account the contribution from nova explosions, assuming that all novae produce the same amount of Li in all events. The contribution from novae is more complex, and we expect it to depend on metallicity and mass, as shown in the works of Kemp et al. (2022) and Kemp et al. (2024). A more complex treatment of novae yields will most likely improve the chemical evolution model in the solar vicinity; however, it is beyond the scope of this paper and will be addressed in a forthcoming work.

The sample of dwarf MS field stars from the Gaia-ESO catalogue is shown in Fig. 8. We also included 275 stars from Bensby & Lind (2018) with the metallicity extending to ∼−2.6 dex. The upper envelope is drawn from the sample of Gaia-ESO data (Magrini et al. 2021) for the comparison. Within the typical uncertainty of A(Li) that is ∼0.1 dex, our model reproduces very well the Spite plateau presented in this sample. The comparison to the defined upper envelope, drawn from the Gaia-ESO data, suggests the model with $^{Li}Y_{Nova} = 2.34 \times 10^{-5}$ $M_\odot$ is the best-fit model. This obtained result is in complete agreement with the GALAH data presented in Fig. 7.

The sample of ∼700 field stars and the averaged Li abundances of 13 open clusters in the solar vicinity (with the galactocentric distance between 7–9 kpc), selected from the catalogue of Romano et al. (2021), are shown in Fig. 9. In the left panel the upper envelope of the field stars in this sample shows a remarkable agreement with the other three catalogues for our best-fit model (model C2.34b). Most clusters have A(Li) within the defined envelope, except for two clusters that are circled in red. However, we also notice their large uncertainties, which are $\sigma_{A(Li)}$ = 0.1 and 0.13 dex for IC 4665 and ρOph, respectively. The right panel of Fig. 9 shows Li abundances as a function of age (in Myr). In this case, we define the upper envelope by considering 20 bins of 500 Myr, starting from 1000 Myr. The black solid line indicates the time when the Sun formed,

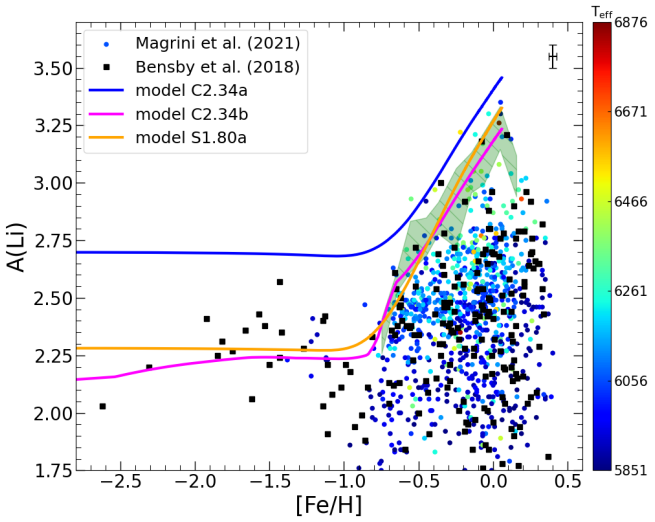

Fig. 8. Li abundance vs metallicity of dwarf MS field stars from the Gaia-ESO (Magrini et al. 2021) and Bensby & Lind (2018) catalogues. The models shown in Fig. 7 are also adopted in this plot. The black error bars indicate the mean uncertainties of the Bensby & Lind (2018) sample.

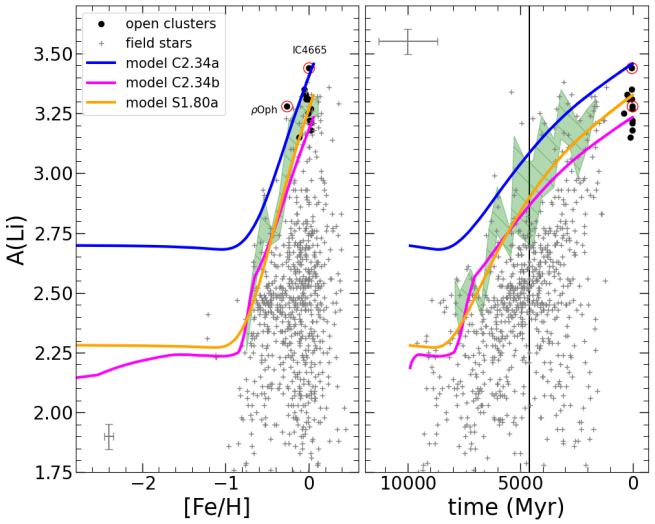

Fig. 9. Li abundances of open clusters and field stars from the Gaia-ESO catalogue (Romano et al. 2021) as a function of metallicity (left panel) and stellar age (right panel). The models shown in Fig. 7 are also adopted in this plot. The grey error bars indicate the mean uncertainties. The shaded area indicates the defined envelope computed from the field stars. The black vertical line in the right panel is for an age of 4.6 Gyr.

4.6 billion years ago. The prediction of the model for the interstellar medium at this age is A(Li) ∼ 3.1 dex, which is 0.2 dex lower than the meteoritic value (A(Li) ∼ 3.3, Lodders et al. 2009). This may indicate that the Sun was born from an inner Galactic region, compared to stars that are present now in the solar vicinity. However, we should clarify two points. First, the uncertainties in the stellar ages prevent us from drawing firm conclusions based on this diagram; second, we consider the yields from novae and their formation channels to be constant. The possible metal and mass dependences could influence and improve the fit as mentioned above. We decide to reserve a more complex treatment for future work. In any case, we find that our model successfully reproduces the Spite plateau and the Li-enrichment in the solar vicinity, showing consistency among four separate catalogues.

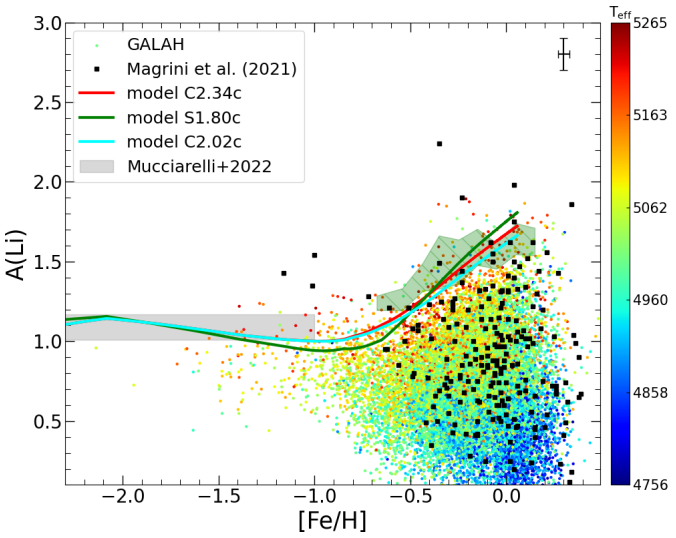

Fig. 10. Li abundance vs metallicity of early RGB stars from the GALAH and Gaia-ESO catalogues, superimposed on our models (solid lines). The grey shaded area is the early RGB plateau from Mucciarelli et al. (2022) (A(Li) = 1.09 ± 0.08). The black error bars indicate the mean uncertainties from the GALAH sample.

In addition, we show in Figs. 7, 8, and 9 the model computed with the Spite plateau value (A(Li) = 2.28 dex) for the sake of comparison. We find agreement with the previous work (Cescutti & Molaro 2019), indicating that a Li yield of $^{Li}Y_{\rm Nova} = 1.8 \times 10^{-5}$ M$_\odot$ would be the best constrained value if the original gas composition is assumed to be the measured value of the Spite plateau. On the other hand, this model predicts a Li abundance in the presolar material that is lower than the measured value (see the discussion of Cescutti & Molaro 2019).

5.2. Early RGB stars

In Sect. 3, we found that stellar models with different masses and metallicities show a possible plateau at the RGB evolution after the 1DU and before the RGB bump. The depletion from the primordial value (A(Li) = 2.69 dex) is ∼1.6 dex at this evolutionary stage.

In Fig. 10, we explore this finding with a sample selected from the GALAH catalogue. Our selected sample was described in Sect. 2. Moreover, for fitting purposes, we excluded the Li-rich stars by using the definition of Magrini et al. (2021). In total, we obtained a sample of 15 297 early RGB stars from the GALAH catalogue, with $-2.14 \leq$ [Fe/H] ≤ 0.48, $4750 \leq T_{\rm eff}/{\rm K} \leq 5270$, and $3 \leq \log g \leq 3.7$. The data shown in Fig. 10 indicate a plateau feature of A(Li) in the low-metallicity region ([Fe/H] ≤ -0.9). At the upper limit, A(Li) is found to be in the range of ∼1.0–1.2 dex. Meanwhile, A(Li) is about 1.8–1.9 dex at [Fe/H] = 0. These typical values are about 1.1–1.3 dex lower than those of the dwarf MS stars in Figs. 7 and 8.

Our chemical evolution model with the depletion from stellar evolution correction (Model C2.34c), assuming A(Li) = 2.69, reproduces very well the early RGB plateau, as indicated in Fig. 10. Moreover, this model, computed with $^{Li}Y_{\rm Nova} = 2.34 \times 10^{-5}$ M$_\odot$, also reproduces very well the upper envelope at the Li-enrichment area. The chemical evolution model, computed with A(Li) = 2.28 dex as the original Li abundance and taking into account the Li depletion between the MS and early RGB phases, is plotted as the solid green line in Fig. 10 and is named model

S1.80c. The prediction made by this model is very similar to that of model C2.34c. This result, on the one hand, prevents us from drawing a firm conclusion about the original Li abundance. On the other hand, it also implies the crucial role of stellar Li depletion correction when studying the galactic Li evolution by using these early RGB stars.

Overall, our chemical evolution model with stellar evolution correction for dwarf MS and early RGB, assuming the primordial Li abundance, achieves a significant agreement with observations. In particular, in the metal-poor region, by taking into account the Li depletion from stellar models, our chemical evolution model (model C2.34b) reproduces very well the Spite plateau, A(Li) ∼ 2.2 dex. At the same time, model C2.34c reproduces very well the plateau of early RGB stars found by Mucciarelli et al. (2022), with an averaged A(Li) ∼ 1.1 dex. In the high-metallicity region, where nova explosions contribute noticeably to the production of Li, our models C2.34b and C2.34c, with $^{Li}Y_{\rm Nova} = 2.34 \times 10^{-5}$ M$_\odot$, reproduce very well the enrichment of galactic Li data in both the early RGB and dwarf MS stars.

We also include the early RGB stars from the catalogue of Magrini et al. (2021) in Fig. 10. At low metallicities, no A(Li) plateau is found in their data. This can be understood from the fact that their catalogue is limited to [Fe/H] > −1 dex. At higher metallicities, our model with stellar Li depletion provides a satisfactory fit to the data.

Finally, we emphasise that this analysis of the early RGB stars is, in fact, the first attempt to study the behaviour of Li due to the 1DU and earlier mixing processes (e.g. convective-driven and atomic diffusion). We rely on the defined upper envelope to obtain our results, as usually done in the literature (Rebolo et al. 1988; Romano et al. 1999; Cescutti & Molaro 2019; Matteucci 2021). However, the presence of Li-rich stars at this evolutionary stage can be problematic for a precise definition of the upper limit (see Casey et al. 2016; Martell et al. 2021, and references therein). A better understanding of Li-rich stars is reserved for future work.

6. Conclusions

We presented in this paper the chemical evolution models for Li in the thin disc of the Milky Way. We adopted data from GALAH DR4 (Wang et al. 2024), the Gaia-ESO surveys (Magrini et al. 2021; Romano et al. 2021), and the sample of Bensby & Lind (2018) for our comparison purposes.

We paid particular attention to two phases of stellar evolution, namely the dwarf MS and early RGB. The data reveal the presence of A(Li) plateaus: the renowned Spite plateau of dwarf MS stars and the early RGB plateau. The second plateau was recently discovered by Mucciarelli et al. (2022) and is also identified in our sample.

The depletion of Li abundance from the primordial value (A(Li) = 2.69 dex) during the PMS evolution of low-mass metal-poor stars due to the efficiency of envelope overshoot, was recently studied by Nguyen et al. (2025a). We investigated the amount of depletion at these two evolutionary stages, the MS and early RGB (when the 1DU is already completed), using their stellar models. In this work, our chemical evolution models assumed that the gas composition has the primordial Li (A(Li) = 2.69 dex) and evolves further with contributions from nova explosions in binary systems. Together with the corrections from stellar models, we found that the model with a total Li yield of $^{Li}Y_{\rm Nova} = 2.34 \times 10^{-5}$ M$_\odot$ produced over the lifetime of a nova, provides the best fit to the observed galactic Li in the thin disc. This constrained yield is in good agreement with the estimated mean value from observations. The model consistently reproduces the Li evolution constructed from both the dwarf MS and the early RGB stars. In this regard, it should be noted that we assumed all novae produce the same amount of Li during their lifetimes. A more complex model, with a dependence of $^{Li}Y_{\rm Nova}$ on mass, metallicity, or delay timescale might help us to have more precise constraints.

In addition, for the sake of completeness, we note that the only interstellar Li measurement in metal-poor material provides a Li abundance in agreement with that of warm halo stars, suggesting that a different solution from stellar model is required to explain the cosmological Li problem (Molaro et al. 2024). In this regard, we should clarify that our attempt in this work – using the correction relative to the primordial value from stellar models to reproduce the Spite plateau – does not rule out the possibility that the interstellar gas composition has the Li abundance measured in dwarf MS stars. This possibility requires more thorough investigation and will be addressed in the coming work.

Finally, we note that Molaro et al. (2020a) studied the Li abundance in the accreted dwarf galaxy Gaia-Sausage-Enceladus, Monaco et al. (2010) in ω Centauri, and Mucciarelli et al. (2014) in the Sagittarius globular cluster M54. In addition, Matteucci et al. (2021) presented chemical evolution models of Li for dwarf spheroidal and ultra-faint galaxies. These authors concluded that the Spite plateau could be a universal feature. This broadens the possibility of testing the internal mixing processes from stellar models, specifically whether they are needed and/or their efficiencies. A comprehensive study on this topic is reserved for future work.

Acknowledgements. The authors thank the anonymous referee for the kind comments and instructive suggestions. We are also thankful to Paolo Molaro for his insight and thorough suggestions, which have helped improve this paper since the first place. This project has received funding from the European Union's Horizon 2020 research and innovation programme under grant agreement No. 101008324 (ChETEC-INFRA). CTN and FR acknowledge the support by INAF Mini grant 2024, "GALoMS – Galactic Archaeology for Low Mass Stars" (1.05.24.07.02). AJK acknowledges support by the Swedish National Space Agency (SNSA). GE acknowledges the contribution of the Next Generation EU funds within the National Recovery and Resilience Plan (PNRR), Mission 4 – Education and Research, Component 2 – From Research to Business (M4C2), Investment Line 3.1 – Strengthening and creation of Research Infrastructures, Project IR0000034 – "STILES – Strengthening the Italian Leadership in ELT and SKA". FR is a fellow of the Alexander von Humboldt Foundation. FR acknowledges support by the Klaus Tschira Foundation. FR and GC acknowledge financial support under the National Recovery and Resilience Plan (NRRP), Mission 4, Component 2, Investment 1.1, Call for tender No. 104 published on 2.2.2022 by the Italian Ministry of University and Research (MUR), funded by the European Union – NextGenerationEU – Project 'Cosmic POT' (PI: L. Magrini) Grant Assignment Decree No. 2022X4TM3H by the Italian Ministry of Ministry of University and Research (MUR). L.M., and G.C. thank I.N.A.F. for the 1.05.23.01.09 Large Grant – Beyond metallicity: Exploiting the full POtential of CHemical elements (EPOCH) (ref. Laura Magrini). A.M., and D.R. acknowledge support from the project "LEGO – Reconstructing the building blocks of the Galaxy by chemical tagging" (PI: A. Mucciarelli). granted by the Italian MUR through contract PRIN 2022LLP8TK_001. Supported by Italian Research Center on High Performance Computing Big Data and Quantum Computing (ICSC), project funded by European Union – NextGenerationEU – and National Recovery and Resilience Plan (NRRP) – Mission 4 Component 2 within the activities of Spoke 3 (Astrophysics and Cosmos Observations). L.M. thank INAF for the support (Large Grants EPOCH and WST), the Mini-Grants Checs (1.05.23.04.02), and the financial support under the National Recovery and Resilience Plan (NRRP), Mission 4, Component 2, Investment 1.1, Call for tender No. 104 published on 2.2.2022 by the Italian Ministry of University and Research (MUR), funded by the European Union – NextGenerationEU – Project 'Cosmic POT' Grant Assignment Decree No. 2022X4TM3H by the Italian Ministry of the University and Research (MUR).

References

Arai, A., Tajitsu, A., Kawakita, H., & Shinnaka, Y. 2021, ApJ, 916, 44
Bensby, T., & Lind, K. 2018, A&A, 615, A151
Bensby, T., Bergemann, M., Rybizki, J., et al. 2019, The Messenger, 175, 35
Bonifacio, P. 2002, A&A, 395, 515
Borisov, S., Prantzos, N., & Charbonnel, C. 2024, A&A, 691, A142
Bressan, A., Marigo, P., Girardi, L., et al. 2012, MNRAS, 427, 127
Buder, S., Sharma, S., Kos, J., et al. 2021, MNRAS, 506, 150
Casey, A. R., Ruchti, G., Masseron, T., et al. 2016, MNRAS, 461, 3336
Cescutti, G., & Molaro, P. 2019, MNRAS, 482, 4372
Charbonnel, C., & Primas, F. 2005, A&A, 442, 961
Charbonnel, C., & Zahn, J. P. 2007, A&A, 467, L15
Coc, A., Vangioni-Flam, E., Descouvemont, P., Adahchour, A., & Angulo, C. 2004, ApJ, 600, 544
Coc, A., Uzan, J.-P., & Vangioni, E. 2014, J. Cosmology Astropart. Phys., 2014, 050
Cyburt, R. H., Fields, B. D., & Olive, K. A. 2003, Phys. Lett. B, 567, 227
Cyburt, R. H., Fields, B. D., Olive, K. A., & Yeh, T.-H. 2016, Rev. Mod. Phys., 88, 015004
Dantas, M. L. L., Smiljanic, R., Romano, D., et al. 2025, A&A, 699, A173
D'Antona, F., & Matteucci, F. 1991, A&A, 248, 62
De Silva, G. M., Freeman, K. C., Bland-Hawthorn, J., et al. 2015, MNRAS, 449, 2604
Della Valle, M., & Izzo, L. 2020, A&A Rev., 28, 3
Ding, M.-Y., Shi, J.-R., Yan, H.-l., et al. 2024, ApJS, 271, 58
Eggenberger, P., Haemmerlé, L., Meynet, G., & Maeder, A. 2012, A&A, 539, A70
Eggenberger, P., Buldgen, G., Salmon, S. J. A. J., et al. 2022, Nat. Astron., 6, 788
Ford, H. C. 1978, ApJ, 219, 595
Franciosini, E., Randich, S., de Laverny, P., et al. 2022, A&A, 668, A49
Fu, X., Bressan, A., Molaro, P., & Marigo, P. 2015, MNRAS, 452, 3256
Fu, X., Romano, D., Bragaglia, A., et al. 2018, A&A, 610, A38
Gao, X., Lind, K., Amarsi, A. M., et al. 2020, MNRAS, 497, L30
Gao, J., Zhu, C., Lü, G., et al. 2024, ApJ, 971, 4
Gao, Q., Shi, J.-R., Yan, H.-L., et al. 2019, ApJS, 245, 33
Greggio, L., & Renzini, A. 1983, A&A, 118, 217
Iliadis, C., & Coc, A. 2020, ApJ, 901, 127
Izzo, L., Della Valle, M., Mason, E., et al. 2015, ApJ, 808, L14
Izzo, L., Molaro, P., Bonifacio, P., et al. 2018, MNRAS, 478, 1601
Izzo, L., Siegert, T., Jean, P., et al. 2025, A&A, 698, A291
Kemp, A. J., Karakas, A. I., Casey, A. R., et al. 2022, ApJ, 933, L30
Kemp, A. J., Karakas, A. I., Casey, A. R., et al. 2024, A&A, 689, A222
Koch, A., Lind, K., Thompson, I. B., & Rich, R. M. 2012, Mem. Soc. Astron. Ital. Suppl., 22, 79
Komatsu, E., Smith, K. M., Dunkley, J., et al. 2011, ApJS, 192, 18
Korn, A. J., Grundahl, F., Richard, O., et al. 2007, ApJ, 671, 402
Kroupa, P. 2001, MNRAS, 322, 231
Lind, K., Primas, F., Charbonnel, C., Grundahl, F., & Asplund, M. 2009, A&A, 503, 545
Lodders, K., Palme, H., & Gail, H. P. 2009, Landolt Börnstein, 4B, 712
Magrini, L., Lagarde, N., Charbonnel, C., et al. 2021, A&A, 651, A84
Martell, S. L., Simpson, J. D., Balasubramaniam, A. G., et al. 2021, MNRAS, 505, 5340
Matteucci, F. 2021, A&A Rev., 29, 5
Matteucci, F., & Greggio, L. 1986, A&A, 154, 279
Matteucci, F., D'Antona, F., & Timmes, F. X. 1995, A&A, 303, 460
Matteucci, F., Molero, M., Aguado, D. S., & Romano, D. 2021, MNRAS, 505, 200
Meynet, G., & Maeder, A. 2002, A&A, 390, 561
Molaro, P., Izzo, L., Mason, E., Bonifacio, P., & Della Valle, M. 2016, MNRAS, 463, L117
Molaro, P., Cescutti, G., & Fu, X. 2020a, MNRAS, 496, 2902
Molaro, P., Izzo, L., Bonifacio, P., et al. 2020b, MNRAS, 492, 4975
Molaro, P., Izzo, L., D'Odorico, V., et al. 2022, MNRAS, 509, 3258
Molaro, P., Izzo, L., Selvelli, P., et al. 2023, MNRAS, 518, 2614
Molaro, P., Bonifacio, P., Cupani, G., & Howk, J. C. 2024, A&A, 690, A38
Monaco, L., Bonifacio, P., Sbordone, L., Villanova, S., & Pancino, E. 2010, A&A, 519, L3
Mucciarelli, A., Salaris, M., Bonifacio, P., Monaco, L., & Villanova, S. 2014, MNRAS, 444, 1812
Mucciarelli, A., Monaco, L., Bonifacio, P., et al. 2022, A&A, 661, A153
Nguyen, C. T., Costa, G., Girardi, L., et al. 2022, A&A, 665, A126
Nguyen, C. T., Bressan, A., Korn, A. J., et al. 2025a, A&A, 696, A136
Nguyen, C. T., Costa, G., Bressan, A., et al. 2025b, A&A, 701, A258
Pitrou, C., Coc, A., Uzan, J.-P., & Vangioni, E. 2021, MNRAS, 502, 2474
Planck Collaboration XVI. 2014, A&A, 571, A16
Prantzos, N. 2012, A&A, 542, A67
Randich, S., Pasquini, L., Franciosini, E., et al. 2020, A&A, 640, L1
Rebolo, R., Molaro, P., & Beckman, J. E. 1988, A&A, 192, 192
Richard, O., Michaud, G., & Richer, J. 2005, ApJ, 619, 538
Romano, D., Matteucci, F., Molaro, P., & Bonifacio, P. 1999, A&A, 352, 117
Romano, D., Matteucci, F., Ventura, P., & D'Antona, F. 2001, A&A, 374, 646
Romano, D., Magrini, L., Randich, S., et al. 2021, A&A, 653, A72
Shafter, A. W. 1997, ApJ, 487, 226
Singh, V., Lahiri, J., Bhowmick, D., & Basu, D. N. 2019, Sov. J. Exp. Theor. Phys., 128, 707
Singh, V., Bhowmick, D., & Basu, D. N. 2024, Astropart. Phys., 162, 102995
Spite, F., & Spite, M. 1982a, A&A, 115, 357
Spite, M., & Spite, F. 1982b, Nature, 297, 483
Tajitsu, A., Sadakane, K., Naito, H., Arai, A., & Aoki, W. 2015, Nature, 518, 381
Tajitsu, A., Sadakane, K., Naito, H., et al. 2016, ApJ, 818, 191
Travaglio, C., Randich, S., Galli, D., et al. 2001, ApJ, 559, 909
Wang, E. X., Nordlander, T., Buder, S., et al. 2024, MNRAS, 528, 5394